Ductile Tearing Instability Assessment of a Cracked Reactor Pressure Vessel Nozzle for Larger Critical Crack Size Compared to the FAD Method

G. Thorwald and J. Wright

Quest Integrity Group, 1965 57th Court North, Suite 100, Boulder, Colorado 80301

Abstract: *The critical flaw size is computed for a cracked nozzle in a reactor pressure vessel using a ductile tearing instability assessment and is compared to the Failure Assessment Diagram method. A material resistance J-R curve and elastic-plastic finite element analyses are used to evaluate the crack stability. The expectation is that the critical crack size will be larger from the tearing instability assessment compared to the FAD assessment, since the rising J-R curve gives higher toughness as stable tearing occurs. A reactor pressure vessel nozzle geometry with a postulated surface crack is used as an example to examine the analysis details and common difficulties encountered when creating the crack model, obtaining the necessary elastic-plastic FEA convergence to compute the J-integral values, and determining the tearing stability point. The non-dimensional tearing modulus plot provides a definite identification of the stability point, which leads to the critical crack size. Reasons for easier elastic-plastic convergence for a tearing stability assessment than for an FAD assessment are examined. Engineers using Abaqus benefit from elastic-plastic FEA of 3D crack meshes by computing the J-integral values needed to assess cracked structural components. When a J-R resistance curve is available, a tearing instability assessment can indicate a larger critical flaw size, which could justify reducing or delaying inspections and could allow for a longer service life in cyclic fatigue before repair or replacement is needed.*

Keywords: *Surface crack, 3D crack mesh, stress intensity, K_I, J-integral, J-R curve, resistance curve, ductile tearing, tearing instability, tied contact, fracture toughness, failure assessment diagram, FAD, Shippingport reactor pressure vessel, RPV, nozzle, Abaqus/Standard*

1. Introduction

Cracked structural components can be evaluated using ductile tearing instability or the Failure Assessment Diagram (FAD). Computing critical flaw sizes helps ensure a damage tolerant structure and in setting appropriate inspection schedules when combined with fatigue analysis. This case study compares the ductile tearing instability and FAD methods using public domain data from the Shippingport reactor pressure vessel (Wikipedia 2015), which is available in an Abaqus™ technical brief (Abaqus 2007). Figure 1 shows a diagram of the vessel with four nozzles in the upper shell and four more nozzles in the bottom head.

The toughness and tensile data for A508 steel are available in ASME standards (API 2007, ASME 2010). The ductile tearing and FAD assessment methodologies are described in the API 579/ASME FFS-1 standard (API 2007), the text book by T.L. Anderson (Anderson 2005), and an assessment example (Thorwald 2011). Since this paper focuses on the ductile tearing analysis method, more details about the FAD method can be found in other examples (Rowson 2011, Tipple 2012, and Thorwald 2015).

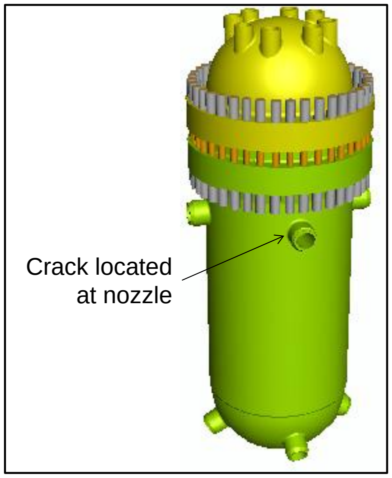

Figure 1. Shippingport reactor pressure vessel.

A postulated surface crack located at an upper nozzle in the shell is analyzed. The vessel has four equally spaced nozzles around the shell; quarter symmetry is used to simplify the vessel model for the cracking analysis. The top head and flange are omitted, since the circumferential flange is much stiffer than the region around the nozzle. Figure 2 shows the quarter vessel geometry, mesh (no crack), and principal stress results due to internal pressure and nozzle pressure thrust. The principal stresses are higher around the base of the nozzle, where a crack could form, giving a good location to examine a postulated crack.

2. Crack meshes

The "user defined geometry" method is used to generate the 3D crack meshes at the nozzle location (FEACrack 2015). Figure 3 shows a close-up of the nozzle and the geometry partition; the gap in the vessel will be filled by the crack meshes. Figure 4 shows the geometry partition and Figure 5 shows the "definition mesh" used to generate the crack meshes in the nozzle. Figure 6 shows an example of a crack mesh (blue) added to the vessel mesh (red). Tied contact connects the meshes and is a crucial feature in Abaqus for this crack meshing approach. The surface cracks have a curved face around the nozzle. To see the crack face mesh pattern, cut-away views are shown in Figure 7. The front part of the vessel shell mesh is hidden, revealing the back crack face and part of the nozzle. The surface crack sizes are given by the crack length, 2*c*, and the crack depth, *a*.

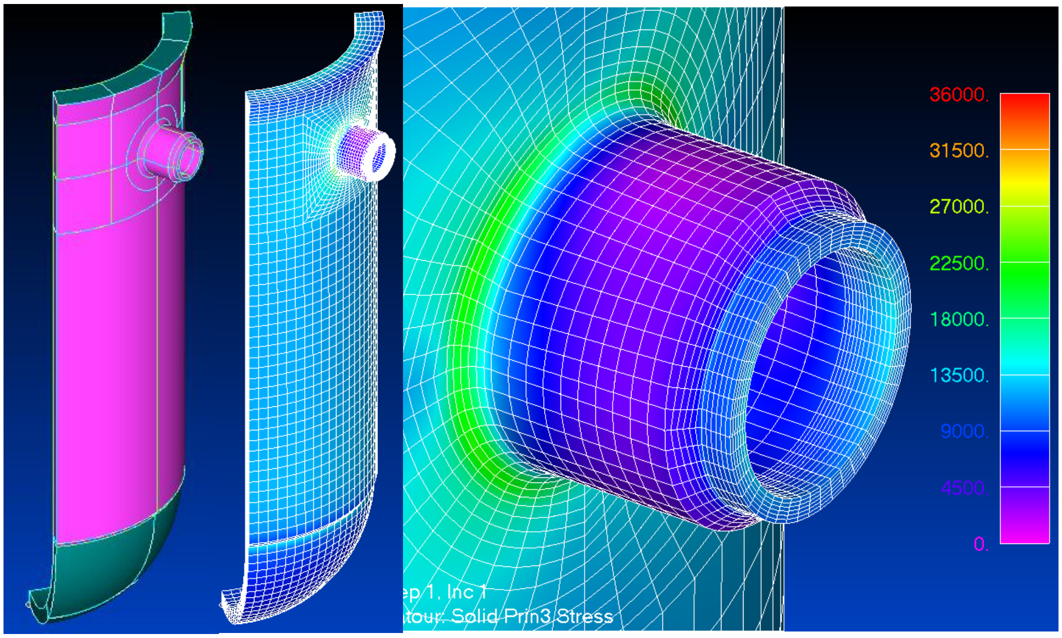

Figure 2. Quarter symmetric vessel geometry, principal stress at nozzle.

A ductile tearing analysis requires a range of crack sizes, so the crack length-to-depth aspect ratio is kept constant at $2c/a = 3$ to create a range of crack sizes. Other crack aspect ratios can be used to develop a full trend of critical crack sizes for shorter to longer crack shapes.

Zooming closer to the upper crack tip, Figure 8 shows the focused mesh pattern (concentric and radial mesh lines from the crack front) needed to compute the J-integral. For elastic-plastic analysis, there is a set of initially coincident nodes for the collapsed brick elements at each crack front position. The coincident nodes can separate as the load is increased, helping to capture crack tip blunting. The number of concentric element groups around the crack front allows separate J-integral contours to be computed and compared to check the contour path dependence.

For the elastic-plastic analysis, the A508 steel material yield strength is 36 ksi, and the tensile strength is 70 ksi (ASME 2010). A Ramberg-Osgood equation is fit to the two tensile values to obtain a stress-strain curve. The Young's modulus, *E*, is 30,000 ksi, and the Poisson's ratio is 0.29. The shell's outside diameter is 125.75 in, and the thickness is 8.375 in.

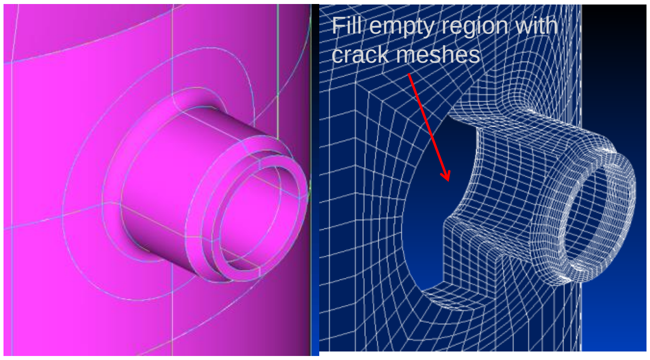

Figure 3. Partition the geometry for the crack mesh region.

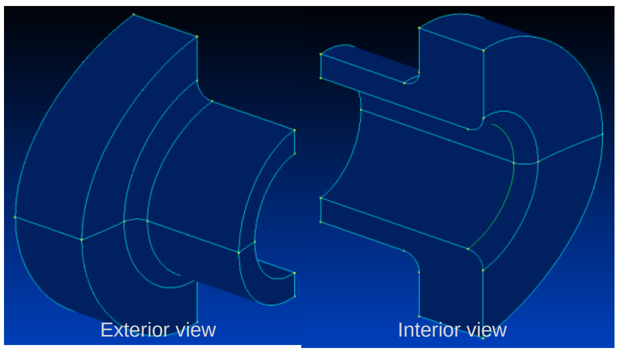

Figure 4. Use half of the nozzle and part of the shell for the crack definition mesh.

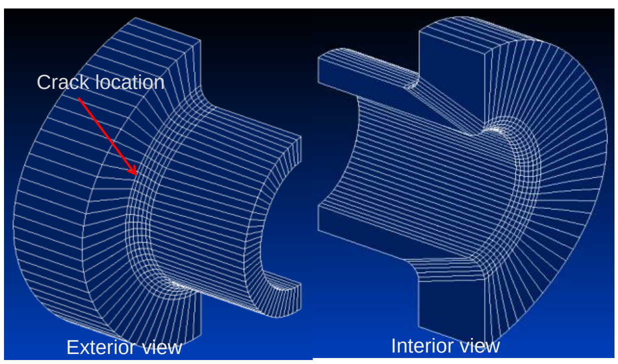

Figure 5. Definition mesh used to create and transform the crack meshes.

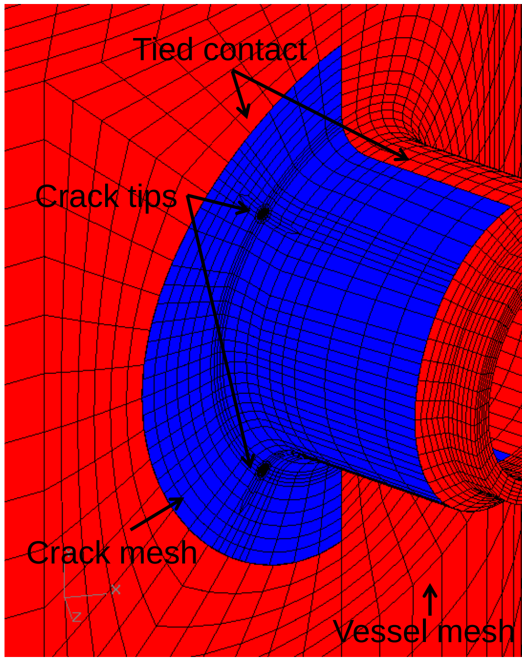

Figure 6. Combined crack mesh (blue) and vessel mesh (red).

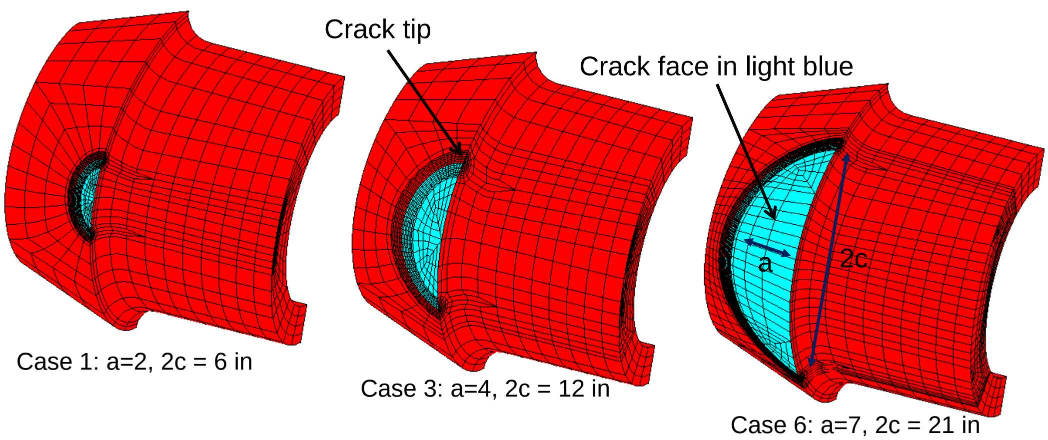

Figure 7. Cut-away view to reveal the surface crack.

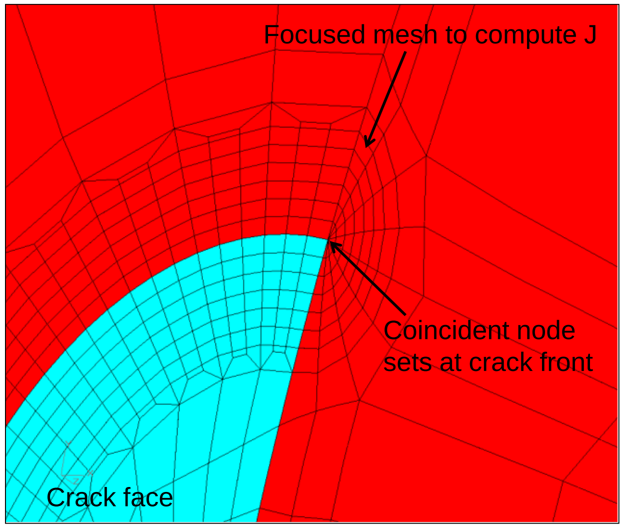

Figure 8. Coincident node sets at the crack front.

3. FEA results

The elastic-plastic analysis for each crack size uses 20 steps for equilibrium convergence and to provide output sets at each pressure load. Using the same pressure load steps for each crack size helps create the ductile tearing assessment plots. Figure 9 shows the principal stress results for the largest and smallest crack sizes; the displacement scale factor is 20 to help show the crack opening.

The crack front J-integral values are shown in Figure 10. The plot x-axis is the crack front node position angle, ϕ, from 0 to π at the crack tips; the center of the plot is at the deepest point of the surface crack, at $\phi=\pi/2$. As the crack size is increased, the J values also increase, which is typical for pressure loading causing tensile stress through the vessel thickness. The crack front J-integral results are used in the ductile tearing instability assessment described in the next section.

4. Ductile tearing instability assessment

The ductile tearing instability analysis method described in the references (Anderson 2005, API 2007, Rowson 2011, and Thorwald 2011) requires a material resistance J-R curve and several crack sizes. The A508 steel J-R curve from API 579 Table F.10 is shown in Figure 11. The J-R curve is given by the power-law Equation 1:

$$J_R = C_T(\Delta a)^{n_T} = C_T(a - a_0)^{n_T} \quad (1)$$

where Δa is the crack extension measured from starting crack size a_0 to the current crack size a, C_T is the tearing coefficient, and n_T is the tearing exponent. For A508 steel at 550 ^{o}F, the coefficient and exponent values are: C_T = 3.443 ksi*in, n_T = 0.329.

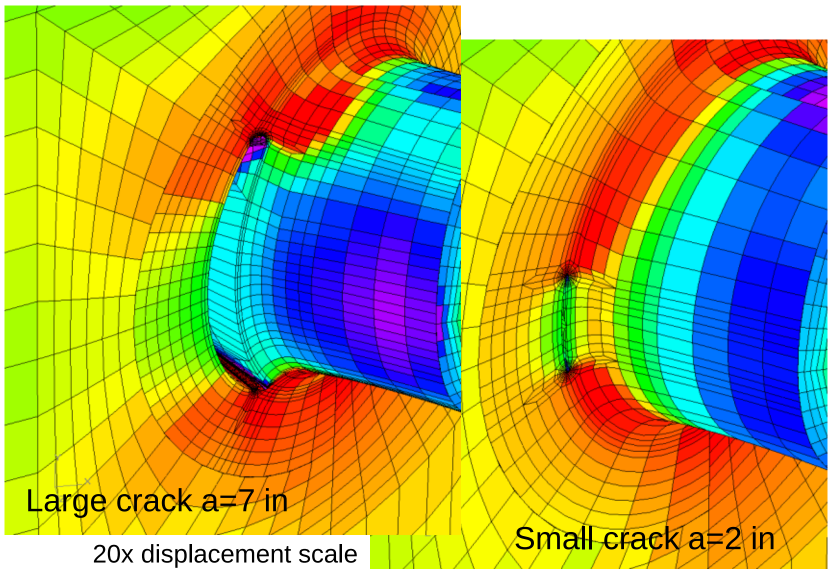

Figure 9. Crack opening and primary stress results.

The 0.2 mm offset line shown in Figure 11 intersects with the J-R curve at the J_{Ic} single toughness value, where crack front blunting gives way to ductile tearing behavior. The slope of the 0.2 mm offset line is given by a constant multiplied by the flow stress. The default constant of 2 is used here, which gives the offset line slope equal to the sum of the yield and tensile strength values. The intersection of the J-R curve and offset line is found by iteration.

For comparison of the A508 J-R curve to other materials, several curves are shown in Figure 12. Most are generic carbon and stainless steels from API 579, and the A53 curve is from material testing (Rowson 2011) according to the ASTM E1820 standard (ASTM 2015).

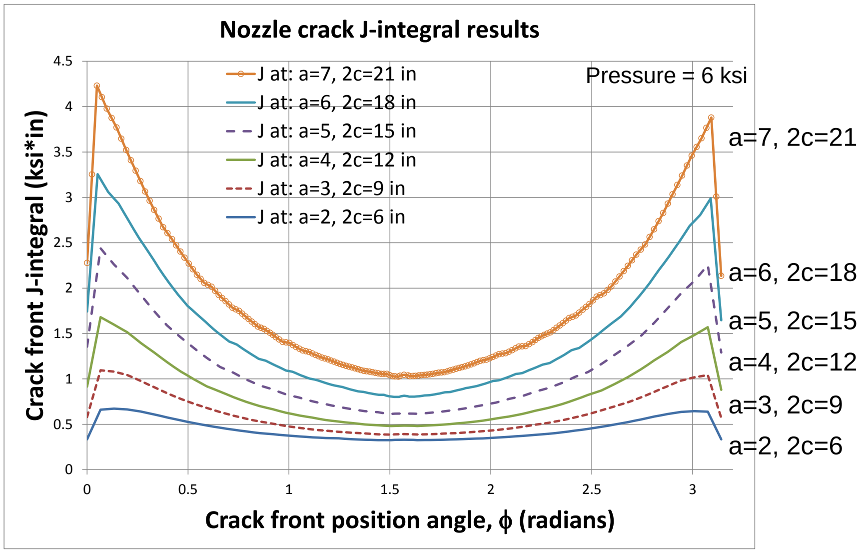

Figure 10. Crack front J-integral results for each crack size.

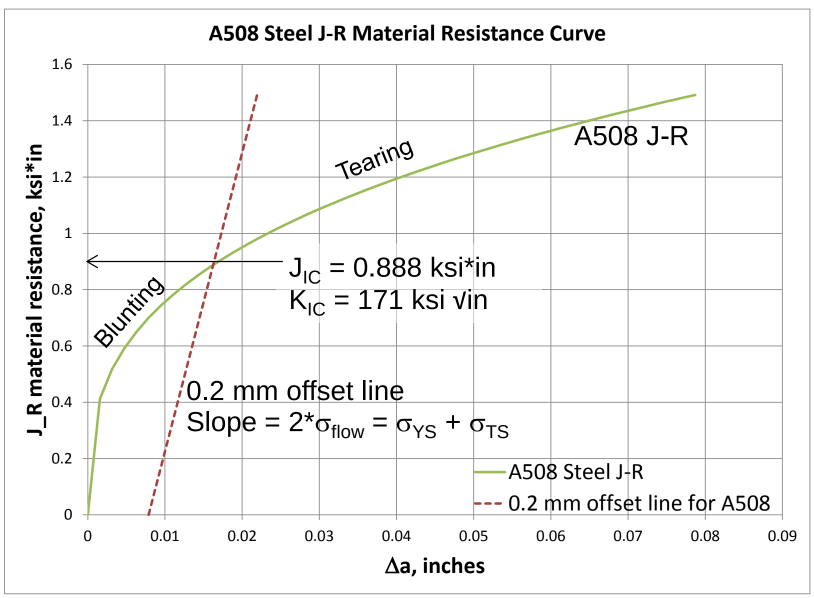

Figure 11. A508 steel J-R resistance curve and single toughness value.

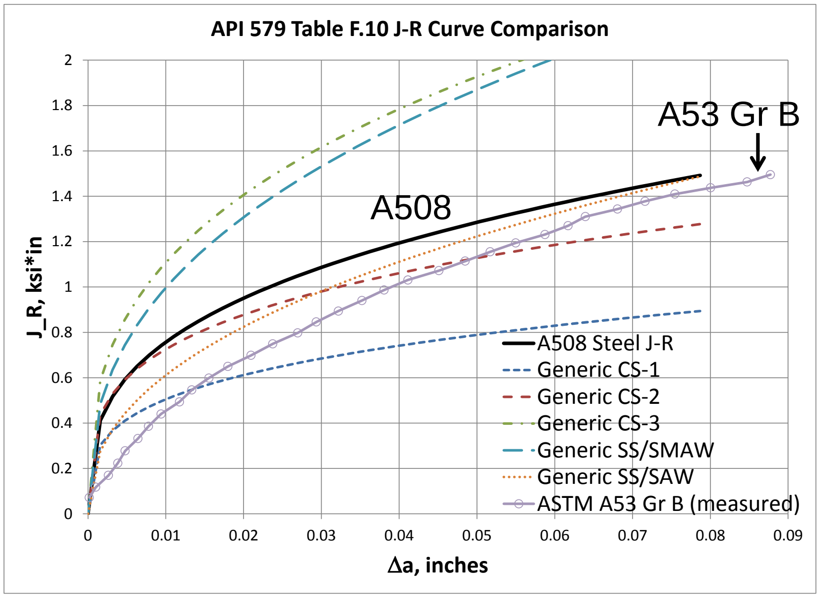

Figure 12. J-R curve comparison.

The ductile tearing instability assessment uses the crack front J-integral values at a given load and compares them to the material resistance J-R curve. Figure 13 shows the crack front maximum J values, which occur near the crack tip, for three pressure load cases versus a range of crack sizes, as represented by the crack depth *a* (plot x-axis) since the 2*c*/*a* aspect ratio is kept constant. The label J_{app} is the "applied" J value from the analysis results. The J_{app} result curves in Figure 13 are obtained by plotting J at the same load value from each crack analysis to get the trend of J versus crack size for comparison to the J-R resistance curve.

A starting point for a ductile tearing assessment would use at least three crack sizes: small, medium, and large, to obtain the J versus *a* trend and compute a tearing modulus. Adding more crack size cases is beneficial to add more data points to the curves, improving the trends and instability assessment.

Imagine the J-R curve in Figure 13 being shifted left and right along the x-axis by varying a_0 until a tangent point is found with a J_{app} curve. For the maximum pressure load case, a tangent point is found at J = 3.7 ksi*in, corresponding to a starting critical crack size of a_0 = 5.2 by $2c_0$ = 15.7 in. If the starting crack size is slightly larger, the crack would be unstable, predicting a failure at this pressure, and the J_{app} and J-R curves would not intersect. If the starting crack size is slightly smaller, the crack would have stable tearing, and the J_{app} and J-R curves would intersect. Note that the two lower pressure load cases intersect the J-R curve and would be considered stable for this starting crack size.

There can be a region of overlap in the J versus *a* curves near the tangent instability point, making visual identification of the tangent point somewhat imprecise. To more precisely locate the tangent instability point, the non-dimensional tearing modulus, *T*, is computed using:

$$T = \frac{E}{\sigma_{YS}^2}\frac{dJ}{da} \quad (2)$$

where E is Young's modulus of elasticity, σ_{YS} is the yield strength, and dJ/da is the derivative of the J_{app} or J-R curve. T_{app} is the tearing modulus computed from J_{app}, and T-R is the tearing modulus computed from the J-R curve.

For the J_{app} curve, a polynomial curve-fit works well to fit the J versus a results and obtain the dJ/da derivative. For the maximum pressure load case, the curve-fit corresponding to the J_{app} top curve in Figure 13 is:

$$J_{app} = 0.00158(a)^3 + 0.0423(a)^2 + 0.231(a) \quad (3)$$

The dJ_{app}/da derivative of the polynomial curve-fit with the exponent values left as multipliers on each term is:

$$\frac{dJ_{app}}{da} = 3 * 0.00158(a)^2 + 2 * 0.0423(a) + 0.231 \quad (4)$$

The T_{app} tearing modulus is computed for the three pressure load cases at each crack size a and plotted versus the corresponding J values for those crack sizes in Figure 14.

The dJ_R/da derivative of the J-R curve power-law in Equation 1 in terms of Δa is:

$$\frac{dJ_R}{da} = n_T C_T (\Delta a)^{n_T} (\Delta a)^{-1} \quad (5)$$

To create the T-R tearing curve it is convenient to put the derivative in terms of J-R, since J is the tearing modulus plot's x-axis. Rearranging Equation 1 to get Δa in terms of J-R and the coefficients to replace the $(\Delta a)^{-1}$ denominator in Equation 5: $\Delta a = (J_R^{1/n_T})/(C_T^{1/n_T})$. Replace the middle two terms of Equation 5 with J-R from Equation 1 to get the T-R tearing modulus equation in terms of J-R and the coefficients but without Δa (Anderson 2005):

$$T_R = \frac{E}{\sigma_{YS}^2}\frac{dJ_R}{da} = \left[\frac{E}{\sigma_{YS}^2}\right]\left[n_T C_T^{1/n_T}\right] J_R^{(n_T-1)/n_T} \quad (6)$$

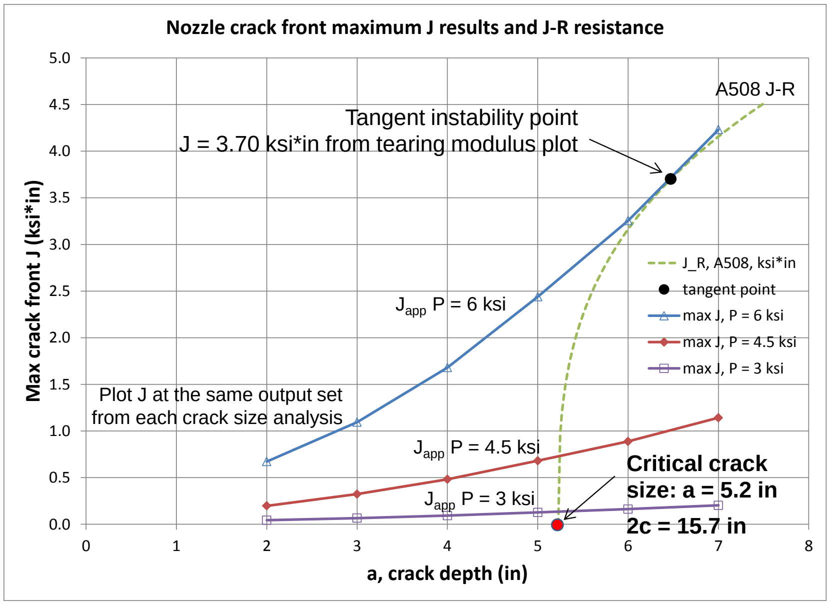

Figure 13. Tangent instability point used to determine critical crack size.

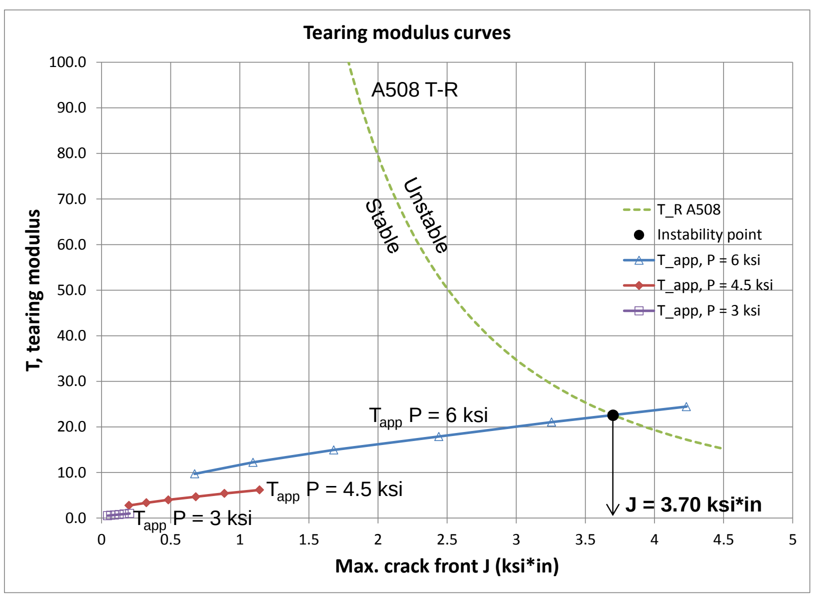

Figure 14. Tearing modulus plot to determine the instability point.

Using the J-R coefficients and material values for A508 steel gives the T-R curve as a function of J:

$$T_R = 326.39J^{-2.0395} \tag{7}$$

The T-R tearing modulus curve is plotted versus J in Figure 14. Points below the T-R curve are stable, and points above the T-R curve are unstable and predict failure. The intersection of the maximum pressure load T_{app} and T-R curves is where the slope of those curves is equal (tangent point), and it gives a more definite instability point than on the J versus *a* plot. For the maximum pressure load case the critical J = 3.70 ksi*in, which is found by iteration.

The critical J value from the tearing modulus curve intersection gives the y-axis value of the tangent instability point in Figure 13. Solving the J_{app} curve-fit Equation 3 by iteration gives the crack size *a* at the tangent point on the J_{app} curve. Finally, Equation 1 is solved iteratively for the starting crack size a_0 using crack size *a* and critical J value at the tangent point.

5. Comparison to the Failure Assessment Diagram method

The FAD method described in the references (API 2007, Anderson 2005, Tipple 2012, and Thorwald 2016) evaluates a cracked structural component using two ratios: Kr and Lr, to give the assessment point location compared to the FAD curve.

The Kr ratio is the crack front stress intensity, K_I, computed using an elastic analysis, divided by the material fracture toughness, K_{Ic}. The Lr ratio is the crack front reference stress computed using the J-integral from an elastic-plastic analysis divided by the yield strength. The reference stress calculation relies on the ratio of the total J divided by an extrapolated elastic J to compute both the Lr ratio and the analysis specific FAD curve.

To compare the FAD method to the ductile tearing instability method, the assessment point is computed for the critical crack size obtained from the tearing instability (*a* = 5.2 by 2*c* = 15.7 in.). The K_{Ic} toughness used to compute the Kr ratio is taken from the J-R curve in Figure 11 at the 0.2 mm offset line. Figure 15 shows that the assessment point (black circle) is outside the FAD curve, indicating that the FAD method is more conservative than the tearing instability method. This is expected since the J-R curve has a rising toughness trend to account for stable ductile tearing before failure. The assessment point is near the right side of the FAD, and is to the right of the A508 recommended Lr,max=1.25 cut-off, indicating that plastic collapse is a possibility. If the default Lr,max cut-off is used, the assessment point is still to the left of that plastic collapse limit.

Another way to compare the assessment methods is to compute the critical flaw size using the FAD method and compare that directly to the critical crack size obtained using tearing instability. Figure 16 shows assessment points for critical crack sizes located on the FAD curves. One choice is to determine the critical flaw size on the analysis specific FAD, and another choice is to determine the critical flaw size on the default API 579 FAD. Both critical crack sizes from the FAD are smaller and more conservative than from the ductile tearing assessment.

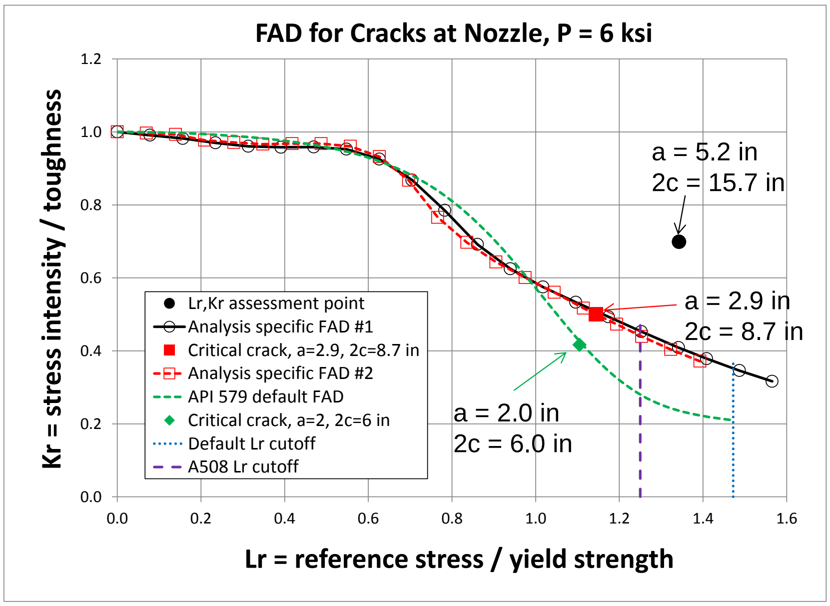

Figure 15. FAD assessment points comparison.

Table 1 compares information needed by both methods, such as elastic-plastic FEA and a range of crack sizes. Both methods have advantages, depending on the material behavior, desired failure assessment, and material data available. The ductile tearing assessment requires the material J-R resistance curve, which may not always be available. A single toughness value or lower-bound toughness may be easier to obtain. The single toughness value used in the FAD method can come from the J-R curve.

The FAD method needs high enough crack front plasticity to complete the reference stress calculations, which can cause FEA convergence difficulties if the estimated maximum loading is too high. Often, the needed maximum load is above the assessment load (a design or operating load) and may take some trial-and-error for adequate J plasticity and convergence. The ductile tearing method only needs convergence up to the assessment load of interest and does not have a crack front plasticity requirement. For smaller cracks or lower loads, the ductile tearing method may be able to indicate quickly that the crack is stable from just a few analysis cases. A separate plastic collapse check is needed for the ductile tearing assessment, especially when the remaining ligament is small, whereas the FAD method has a built-in plastic collapse check at the Lr_{max} cutoff.

The FAD and ductile tearing methods from API 579 are single parameter assessment methods using K or J to characterize the crack front. In some crack cases a two parameter approach may be needed to characterize the crack front, such as also computing the T-stress. ASTM 2899 [13] uses a function of J and T-stress to determine the instability location along the crack front, which could be used to extend this analysis.

Table 1. Analysis method comparison.

Ductile tearing instability assessment	Failure Assessment Diagram
A. Need several crack sizes to compute the tearing modulus curves to get critical flaw size B. Use J-R resistance curve when material behavior is ductile C. Can have easier elastic-plastic FEA convergence to the assessment load D. Can have fewer load steps and output sets; output needed just at the assessment load cases E. Can give larger critical flaw size; may allow for longer service life or fewer inspections F. Check for plastic collapse separately, especially for larger flaw sizes	1. Need several crack sizes to determine the critical flaw size on the FAD curve 2. Use a single toughness value for Kr ratio; can evaluate brittle or ductile material behavior 3. A separate elastic analysis is needed to compute stress intensity K to get Kr 4. High applied maximum loading needed to get sufficient crack front plasticity could lead to convergence issues 5. Need 20 to 30 or more output sets for the reference stress and custom FAD post processing calculations 6. May give a conservative critical crack size compared to ductile tearing 7. Plastic collapse check built into Lr_{max}

6. Summary

The ductile tearing instability assessment and Failure Assessment Diagram methods were compared by computing a critical flaw size of a postulated crack in the Shippingport reactor pressure vessel. Elastic-plastic FEA using 3D crack meshes computed the crack front J-integral values needed for both methods. A range of crack sizes was used in both methods to determine the critical flaw size. The tearing instability assessment uses the J-R material resistance curve, and the FAD method uses a single toughness value. In this example the tearing instability gave a larger critical crack size compared to the FAD method. Both methods have advantages depending on the material behavior, the desired failure assessment method, and the material data available.

7. References

1. Abaqus/Standard™ version 6.14-1, Dassault Systémes Simulia Corp., Providence, RI.
2. Abaqus Technology Brief, TB-060ARCAE-1, "Coupled Thermal-Structural Analysis of the Shippingport Nuclear Reactor Using Adaptive Remshing in Abaqus/CAE," Revised April 2007, URL: http://www.3ds.com//fileadmin/PRODUCTS/SIMULIA/PDF/tech-briefs/En-Coupled-Thermal-Structural-Analysis-Shippingport-06.pdf, accessed Oct. 2015.
3. Anderson, T. L., Fracture Mechanics, Fundamentals and Applications, 3rd ed., 2005, CRC Press, Taylor & Francis Group, Section 7.4, Section 9.3.3, and Equations 9.51 and 9.52.
4. API 579-1/ASME FFS-1 2007 Fitness-for-Service, Table F.10, page F-67 and Part 9, June 5, 2007, American Petroleum Institute and American Society of Mechanical Engineers, API Publishing Services, 1220 L Street, N.W., Washington, D.C. 20005.
5. ASME Boiler and Pressure Vessel Code, Section II, Part D 2010 Table U, p. 464 and Table Y-1, p. 544, American Society of Mechanical Engineers, Three Park Ave, New York, NY 10016.
6. ASTM E1820-15, "Standard Test Method for Measurement of Fracture Toughness," ASTM International, 2015, 100 Barr Harbor Drive, PO Box C700, West Conshohocken, PA 19428.
7. FEACrack™, Version 3.2.27, 2015, Quest Integrity USA, 1965 57th Court North Suite 100, Boulder, Colorado 80301, www.questintegrity.com.
8. Rowson, Q., and M. Rock, "Comparison Between Ductile Tearing Analysis and Linear Elastic Fracture Mechanics Analysis," NAFEMS World Congress, May 2011, Boston, MA.
9. Thorwald, G., and M. Rock, "Ductile Tearing Analysis of a Custom Pipe to Flange Nozzle Using 3D Crack Meshes," NAFEMS World Congress, May 2011, Boston, MA.
10. Thorwald, G., and L. Parietti, "Leak-Before-Break Assessment of a Cracked Reactor Vessel Using 3D Crack Meshes," Proceedings of the ASME 2016 Pressure Vessels and Piping Conference, PVP2016, July 17-21, 2016, paper no. PVP2016-63910.
11. Tipple, C., and G. Thorwald, "Using the Failure Assessment Diagram Method with Fatigue Crack Growth to Determine Leak-before-Rupture," SIMULIA Community Conference, May 2012, Providence, RI.
12. Wikipedia, "Shippingport Atomic Power Station," URL: https://en.wikipedia.org/wiki/Shippingport_Atomic_Power_Station, accessed Dec. 17, 2015.
13. ASTM E2899-13, "Standard Test Method for Measurement of Initiation Toughness in Surface Cracks Under Tension and Bending," ASTM International, 2013, 100 Barr Harbor Drive, PO Box C700, West Conshohocken, PA 19428.